Measurement of the Homogeneous Contact of a Unitary Fermi Gas

Yoav Sagi, Tara E. Drake, Rabin Paudel, and Deborah S. Jin

Phys. Rev. Lett. **109**, 220402 — Published 27 November 2012

DOI: 10.1103/PhysRevLett.109.220402

Measurement of the Homogeneous Contact of a Unitary Fermi gas

Yoav Sagi, Tara E. Drake, Rabin Paudel, and Deborah S. Jin*
JILA, National Institute of Standards and Technology and the University of Colorado, and the Department of Physics, University of Colorado, Boulder, CO 80309-0440, USA
(Dated: October 23, 2012)

By selectively probing the center of a trapped gas, we measure the local, or homogeneous, contact of a unitary Fermi gas as a function of temperature. Tan's contact, C, is proportional to the derivative of the energy with respect to the interaction strength, and is thus an essential thermodynamic quantity for a gas with short-range correlations. Theoretical predictions for the temperature dependence of C differ substantially, especially near the superfluid transition, T_c, where C is predicted to either sharply decrease, sharply increase, or change very little. For $T/T_F > 0.4$, our measurements of the homogeneous gas contact show a gradual decrease of C with increasing temperature, as predicted by theory. We observe a sharp decrease in C at $T/T_F = 0.16$, which may be due to the superfluid phase transition. While a sharp decrease in C below T_c is predicted by some many-body theories, we find that none of the predictions fully accounts for the data.

PACS numbers: 03.75.Ss,67.85.Lm

The collective behavior of an ensemble of strongly interacting fermions is central to many physical systems including liquid ^{3}He, high-T_c superconductors, quark-gluon plasma, neutron stars, and ultracold Fermi gases. However, theoretical understanding of strongly interacting fermions is challenging due to the many-body nature of the problem and the fact that there is no obvious small parameter for a perturbative analysis. Therefore, in order to establish the validity and applicability of theoretical approaches, it is essential to compare them against experimental results. Ultracold atomic Fermi gases are ideal for this purpose, as they provide excellent controllability, reproducibility, and unique detection methods [1, 2]. In particular, changing the magnetic field in the vicinity of a Feshbach resonance enables precise control of the interactions, which are characterized by the s-wave scattering length [3]. On resonance, the scattering length diverges and the behavior of the unitary gas no longer depends on it. Testing theories in this regime is especially desirable.

An outstanding issue for the unitary Fermi gas is the nature of the normal state just above the transition temperature, T_c, for a superfluid of paired fermions. Some theories of strongly interacting Fermi gases (BCS-BEC crossover theories) predict that the normal state is not the ubiquitous Fermi liquid but instead involves incoherent fermion pairing (preformed pairs) in what has been termed the pseudogap state [4]. It has been suggested that the pseudogap state affects the temperature dependence of a quantity called Tan's contact [5]. The contact, which is a measure of the short-range correlation function, has been shown to be an essential thermodynamic parameter for ensembles with short-range interactions [6–11]. The contact connects many seemingly unrelated quantities through a set of universal relations that are valid for any temperature, any interaction strength, and any phase of the system. While the value of the contact, as well as many of these relations, were tested successfully at low temperature [12–15], there are significant discrepancies among theories on how the contact of a unitary homogeneous Fermi gas depends on temperature, especially around T_c [5, 16–19]. The temperature dependence of the contact was recently measured for a trapped unitary Fermi gas [20]. However, for the trapped gas, averaging over the inhomogeneous density distribution washes out any temperature-dependent features, and the measurement was unable to differentiate between theoretical models. Here we present a measurement of the homogeneous contact, which can be directly compared to the predictions of different many-body theories.

We perform the experiments with an optically trapped ultracold gas of ^{40}K atoms in an equal mixture of the $|f, m_f\rangle = |9/2, -9/2\rangle$ and $|9/2, -7/2\rangle$ spin states, where f is the quantum number denoting the total atomic spin and m_f is its projection [21]. We determine the contact by combining rf spectroscopy with a recently demonstrated technique to probe the local properties of a trapped gas [22]. Probing atoms locally is accomplished by intersecting two perpendicularly propagating hollow light beams that optically pump atoms at the edge of the cloud into a spin state that is dark to the detection (see figure 1a). The experimental sequence is depicted in figure 1b. The magnetic field is ramped adiabatically to the Feshbach resonance and kept at this value for 2 ms before abruptly shutting off the trapping potential. Before the potential is shut off, the hollow beams are pulsed on, followed by the rf pulse, which transfers a small fraction of the atoms in the occupied $|9/2, -7/2\rangle$ state to the initially unoccupied $|9/2, -5/2\rangle$ state (which is weakly interacting with the other two spin states). We detect these atoms using absorption imaging after 3 ms of expansion. The temperature of the gas is varied by changing the final depth of the optical dipole trap in the evaporation process [21]. The number of atoms per spin state after the evaporation ranges from $50,000$ to $220,000$. For the data presented in this paper, the radial trapping fre-

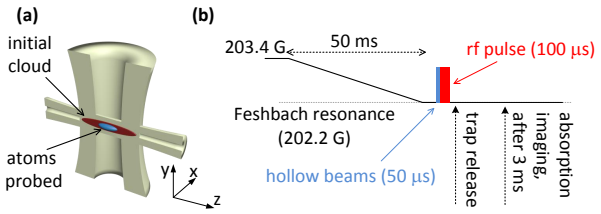

FIG. 1. Schematics of the experiment. **(a)** We probe the center of the gas by optically pumping the outer parts of the cigar-shaped cloud to a dark state using two intersecting second-order Laguerre-Gaussian beams [22]. By changing the beams' power, we control the fraction of atoms probed. The power of the two beams is set such that the number of atoms optically pumped by each beam is about the same. **(b)** The magnetic field is ramped from 203.4 G, where the atoms are initially prepared, to the Feshbach resonance. The hollow light beams are turned on 280 μs before trap release; initially, the beam that propagates perpendicular to the long axis of the cloud is pulsed on for 10 μs followed by 40 μs of the second beam. The line shape is measured using an rf pulse with a total duration of 100 μs and a gaussian field envelope with $\sigma = 17\,\mu s$, centered 180 μs before trap release. The cloud expands for 3 ms before being detected by absorption imaging. To improve the signal-to-noise ratio, we remove the remaining atoms from the $|9/2,-9/2\rangle$ and $|9/2,-7/2\rangle$ states and then transfer the outcoupled atoms in the $|9/2,-5/2\rangle$ state to the $|9/2,-9/2\rangle$ state, where we image on the cycling transition [23].

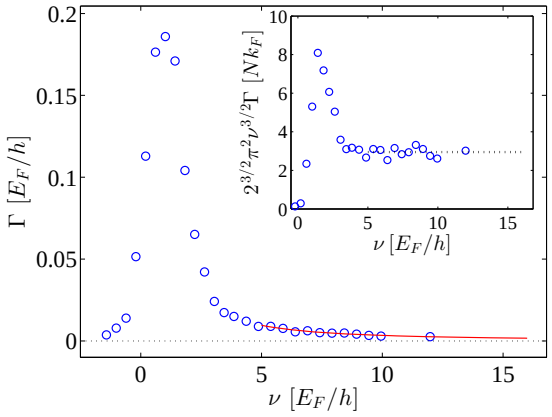

FIG. 2. An rf line shape for the unitary Fermi gas at $T/T_F = 0.25$ with 30% of the atoms probed. The solid (red) line is a fit to Eq.(1) with the normalization $\int_{-\infty}^{\infty}\Gamma(\nu)\mathrm{d}\nu = 1/2$, due to the $50\% - 50\%$ spin mixture. The inset shows the same data multiplied by $2^{3/2}\pi^2\nu^{3/2}$. We make sure the rf pulse induces only a small perturbation, by setting its power to well below the value where we see the onset of saturation of the number of outcoupled atoms [24]. The measurement at different frequencies is done with different rf powers, and when analyzing the data, we linearly scale the measured number of atoms outcoupled at each frequency to correspond to a common rf power.

quency, ω_r, ranges from $2\pi\times 200$ Hz to $2\pi\times 410$ Hz, while the axial trapping frequency, ω_z, ranges from $2\pi\times 19$ Hz to $2\pi\times 25$ Hz.

The contact is extracted from a measurement of the rf line shape $\Gamma(\nu)$ [12], where $\Gamma(\nu)$ is the rate of atoms transferred from one of the two interacting spin states to a third state, by an rf pulse centered at a frequency detuning ν. A representative data set, where the hollow light beams were used to select the central 30% of the atom cloud, is shown in figure 2. For each line shape, we take data at 30 different detunings between -16 kHz and $+116$ kHz, where $\nu = 0$ is defined as the single-particle transition frequency between the $|9/2,-7/2\rangle$ and $|9/2,-5/2\rangle$ states (measured for a spin polarized gas in the $|9/2,-7/2\rangle$ state). The highest frequency typically corresponds to approximately $13\,E_F/h$. The high frequency tail of the rf line shape is predicted to scale as $\nu^{-3/2}$, with the contact connecting the amplitude of the high frequency tail through (see Ref. [11] and references therein):

$$\frac{\Gamma(\nu)}{\int_{-\infty}^{\infty}\Gamma(\nu')\mathrm{d}\nu'} = \frac{C/(Nk_F)}{\sqrt{2}\pi^2\nu^{3/2}} \quad \text{for } \nu\to\infty \qquad (1)$$

where N is the total number of atoms, and $\hbar k_F$ is the Fermi momentum, and ν is the rf detuning in units of the Fermi energy, E_F/h, with h being the Planck constant ($2\pi\hbar \equiv h$). The inset of figure 2 shows $\Gamma(\nu)$ multiplied by $2^{3/2}\pi^2\nu^{3/2}$, where we observe a plateau for frequencies higher than $5\,E_F/h$. We extract the contact by fitting the measured $\Gamma(\nu)$ for $\nu > 5\,E_F/h$ to Eq.(1) (solid line in figure 2). For the normalization, we integrate the line shape, including the tail, up to $\nu = \hbar/mr_{\mathrm{eff}}^2$, where r_{eff} is the effective range of the interaction [3] (which is approximately $300E_F/\hbar$).

The main result of the paper, namely the homogeneous contact versus the temperature, is presented in figure 3. The contact is normalized to the average k_F of the probed sample, and temperature is given in terms of T/T_F, with T_F being the average Fermi temperature of the probed sample (we explain later how we determine these quantities). The data shows a monotonic decrease of the contact with increasing temperature from a maximum value of 3.3 Nk_F. For $T/T_F = 0.16$, at the edge of our experimentally attainable temperatures, we observe a sharp decrease of the contact to about 2.6 Nk_F. In figure 3, we compare our data with several theoretical models [18] and a quantum Monte-Carlo (QMC) simulation [19]. The many-body theories are in the framework of the t-matrix approximation, differing by their choice of the diagrammatic expansion, the particle-particle propagator, and the self-energy. For $T/T_F > 0.4$, the differences between the theoretical models are small, and the predictions all lie within the uncertainty of the data. As expected, at higher temperatures ($T/T_F > 1$), we find good agreement with the virial expansions [18] (see inset

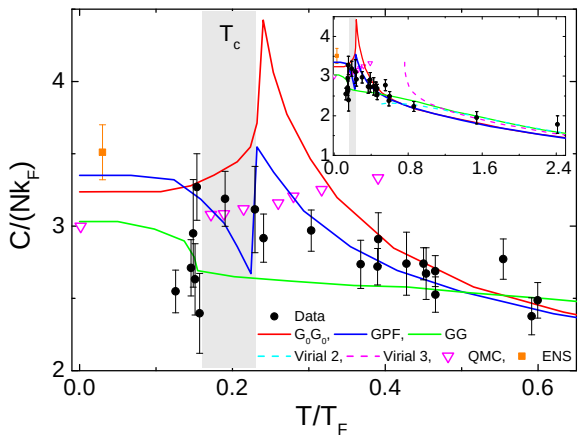

FIG. 3. The contact of a nearly homogeneous sample (about 30% of the trapped atoms probed), versus T/T_F at unitarity (black circles). The shaded area marks the superfluid phase transition, with some uncertainty in its exact position ($T_c/T_F = 0.16 - 0.23$) [25]. As a comparison, we plot the gaussian pair-fluctuation NSR model (GPF) [18], the self-consistent t-matrix model (GG) [25], the non-self-consistent t-matrix model (G_0G_0) [5], the 2nd and 3rd order virial expansion [18], a quantum Monte-Carlo calculation (QMC) [19], and the contact extracted from a thermodynamic measurement done at ENS [26]. The error bars represent one standard deviation. The inset shows the high temperature behavior of the contact, where we find good agreement with the virial expansion.

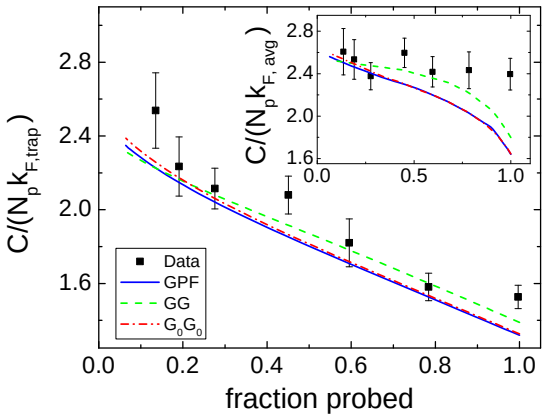

FIG. 4. Contact versus the fraction of atoms probed for a gas with $T/T_F = 0.46$ at the center of the cloud. In the main plot, the measured contact (squares) is normalized in respect to the trap k_F, and is compared to the predictions of several theoretical models (lines) using the local density approximation. The measured contact increases as we probe fewer atoms at the cloud center, where the local density is largest. The inset shows the contact normalized by the average k_F of the probed atoms (squares), compared to theoretical predictions of the homogeneous contact at the average T/T_F (lines).

of figure 3). For $T/T_F < 0.4$, our data do not agree fully with any of the many-body theories. It is worth noting, however, that two of the theories (GPF and G_0G_0) predict a higher value for the contact above the superfluid phase transition than below, which may be consistent with observed sharp decrease near $T/T_F = 0.16$. We note that the predicted T_c/T_F has some uncertainty, as indicated by the shaded region in figure 3. The non-self-consistent t-matrix model (G_0G_0) predicts an enhancement of about 50% in the value of the contact around T_c [5], which the data do not show. We also do not observe an increasing trend in the contact for $T > T_c$, in contrast to a recent QMC simulation [19].

As can be seen from Eq.(1), the contact is naturally normalized by Nk_F, and the detuning by the Fermi energy. However, a question which arises is how to define E_F in our experiment. For a harmonically trapped gas, E_F is defined in terms of the trap parameters $E_{F,\mathrm{trap}} = \hbar(\omega_r^2\omega_z)^{1/3}(6N)^{1/3}$. On the other hand, the Fermi energy of a homogeneous gas is given in terms of its density (in one spin state), n: $E_{F,\mathrm{hom}} = \frac{\hbar^2}{2m}(6\pi^2 n)^{2/3}$. In our experiment, as we increase the power of the hollow light beams, we probe a smaller portion of the gas that is more homogeneous. The relevant Fermi energy, which we use in figures 2 and 3, is therefore the average of the local (homogeneous) Fermi energy: $E_{F,\mathrm{avg}} = \frac{\hbar^2}{2mN_p}\int P(\mathbf{r})n(\mathbf{r})[6\pi^2 n(\mathbf{r})]^{2/3}\mathrm{d}^3\mathrm{r}$, where $P(\mathbf{r})$ is the detection probability after optical pumping, and $N_p = \int P(\mathbf{r})n(\mathbf{r})\mathrm{d}^3\mathrm{r}$ is the number of atoms probed.

The average local Fermi energy can be obtained from the density distribution of the atoms, $n(\mathbf{r})$, and the detection probability, $P(\mathbf{r})$. We measure $n(\mathbf{r})$ by turning the trap off, without applying the hollow light beams, and imaging the cloud after 4 ms of expansion at the resonance. To determine the density distribution in trap, we fit the distribution measured after expansion and rescale the dimensions back to $t = 0$, assuming hydrodynamic expansion [24, 27]. For the fit, we use the Thomas-Fermi distribution, which is known to fit the data well [2].

We obtain $P(\mathbf{r})$ using a model of the optical pumping by the hollow light beams [22]. In the model, we assume that atoms that scatter a single photon are transferred to the dark state, and we account for the attenuation of the hollow light beams as they propagate through the cloud. For a given $n(\mathbf{r})$, the propagation model gives us $P(\mathbf{r})$ after the consecutive application of the two hollow light beams. We note that the results presented in figure 3 are not sensitive to the details of the model [24].

In figure 4, we show the contact at $T/T_F = 0.46$ as a function of the fraction of atoms probed, which is varied by changing the intensity of the hollow light beams. The main part of figure 4 shows the contact per particle in units of $k_{F,\mathrm{trap}}$ in order to show the change in the measured signal. We find that the signal increases as we probe fewer atoms near the center of the trapped gas. We compare our results with several theo-

retical models, where the model lines are calculated by $C_{\rm trap}^{\rm model} = \frac{1}{N_p k_{F,\rm trap}} \int P(\mathbf{r}) n(\mathbf{r}) C_{\rm hom}^{\rm model}[T/T_F(\mathbf{r})] k_F(\mathbf{r}) {\rm d}^3{\rm r}$, with $C_{\rm hom}^{\rm model}(T/T_F)$ being the model prediction for a homogeneous contact (normalized to Nk_F), $T_F(\mathbf{r}) = E_F(\mathbf{r})/k_B$ is the local Fermi temperature, and k_B is the Boltzmann constant. We find good agreement of the data with the models.

In the inset of figure 4, we plot the contact divided by the average local k_F, defined in the same way as in figure 3. For comparison, we also plot theory predictions for the homogeneous contact at the average T/T_F, $C_{\rm hom}^{\rm model}(\langle T/T_F\rangle)$, where the notation $\langle\rangle$ stands for density-weighted averaging. A reasonable criterion for homogeneity is when $C_{\rm hom}^{\rm model}(\langle T/T_F\rangle) \approx \langle C_{\rm hom}^{\rm model}(T/T_F)\rangle$. When the fraction of the atoms probed is less than 30% we find that this approximation holds to better than 2% [24]. When probing 30% of the atoms, we calculate that the rms spread in the local T_F has been reduced to about 20%. We find that the data for $T/T_F = 0.46$ and fractions lower than 30% agree with theory predictions for a homogeneous gas (see inset of figure 4).

Lastly, we describe our determination of the temperature of the gas at unitarity. Thermometry of a strongly interacting gas is not trivial, and different groups have used various techniques, including thermometry with a minority component [26], measurement of the energy versus entropy relation [28], and an empirical temperature extracted from fitting the cloud to a Thomas-Fermi distribution [20]. We base our thermometry on a measurement of the release energy of the gas and the recently reported equation of state [29]. We determine the release energy by taking an image of cloud after 4 ms of expansion at unitarity. Knowing our trapping potential, the equation of state, and the generalized virial theorem at unitarity [28], we are left with only the temperature, T, as a free parameter in the calculation of the release energy. We find T by matching the calculated energy to the measured one [24]. We estimate that the one sigma uncertainty in the temperature is 5%. When reporting T/T_F in figure 3, we use $T_F = E_{F,\rm avg}/k_B$.

In summary, we have presented a measurement of the homogeneous contact of a unitary Fermi gas versus temperature. Our measurement is based on a novel technique that allows us to probe local properties of the cloud. Our data show good agreement with theory predictions for $T/T_F > 0.4$, but at lower temperatures no single prediction fully agrees with the data. Furthermore, the data do not show an enhanced narrow peak around $\rm T_c$, which was predicted to exist due to pair fluctuation in a pseudogap phase. To provide additional insight into the nature of the normal state of the unitary Fermi gas, it will be interesting to test directly the pseudogap pairing instability by combining our probing technique with momentum-resolved rf spectroscopy [21, 23].

We acknowledge funding from the NSF and NIST.

* Electronic address: jin@jilau1.colorado.edu

[1] C. A. Regal and D. S. Jin, Adv. Atom. Mol. Opt. Phys. **54**, 1 (2006).

[2] W. Ketterle and M. W. Zwierlein, in *Proceedings of the International School of Physics "Enrico Fermi", Course CLXIV*, edited by M. Inguscio, W. Ketterle, and C. Salomon (IOS Press, Amsterdam, 2008).

[3] C. Chin, R. Grimm, P. Julienne, and E. Tiesinga, Rev. Mod. Phys. **82**, 1225 (2010).

[4] Q. Chen, J. Stajic, S. Tan, and K. Levin, Physics Reports **412**, 1 (2005).

[5] F. Palestini, A. Perali, P. Pieri, and G. C. Strinati, Phys. Rev. A **82**, 021605 (2010).

[6] S. Tan, Ann. Phys. **323**, 2952 (2008).

[7] S. Tan, Ann. Phys. **323**, 2971 (2008).

[8] S. Tan, Ann. Phys. **323**, 2987 (2008).

[9] E. Braaten, D. Kang, and L. Platter, Phys. Rev. Lett. **100**, 205301 (2008).

[10] S. Zhang and A. J. Leggett, Phys. Rev. A **79**, 023601 (2009).

[11] E. Braaten, in *The BCS-BEC Crossover and the Unitary Fermi Gas*, Lecture Notes in Physics, Vol. 836, edited by W. Zwerger (Springer Berlin / Heidelberg, 2012) pp. 193–231.

[12] J. T. Stewart, J. P. Gaebler, T. E. Drake, and D. S. Jin, Phys. Rev. Lett. **104**, 235301 (2010).

[13] E. D. Kuhnle, H. Hu, X.-J. Liu, P. Dyke, M. Mark, P. D. Drummond, P. Hannaford, and C. J. Vale, Phys. Rev. Lett. **105**, 070402 (2010).

[14] G. B. Partridge, K. E. Strecker, R. I. Kamar, M. W. Jack, and R. G. Hulet, Phys. Rev. Lett. **95**, 020404 (2005).

[15] F. Werner, L. Tarruell, and Y. Castin, Eur. Phys. J. B **68**, 401 (2009).

[16] Z. Yu, G. M. Bruun, and G. Baym, Phys. Rev. A **80**, 023615 (2009).

[17] T. Enss, R. Haussmann, and W. Zwerger, Ann. Phys. **326**, 770 (2011).

[18] H. Hu, X.-J. Liu, and P. D. Drummond, New J. Phys. **13**, 035007 (2011).

[19] J. E. Drut, T. A. Lähde, and T. Ten, Phys. Rev. Lett. **106**, 205302 (2011).

[20] E. D. Kuhnle, S. Hoinka, P. Dyke, H. Hu, P. Hannaford, and C. J. Vale, Phys. Rev. Lett. **106**, 170402 (2011).

[21] J. T. Stewart, J. P. Gaebler, and D. S. Jin, Nature **454**, 744 (2008).

[22] T. E. Drake, Y. Sagi, R. Paudel, J. T. Stewart, J. P. Gaebler, and D. S. Jin, Phys. Rev. A **86**, 031601 (2012).

[23] J. P. Gaebler, J. T. Stewart, T. E. Drake, D. S. Jin, A. Perali, P. Pieri, and G. C. Strinati, Nat. Phys. **6**, 569 (2010).

[24] See Supplemental Material at http://link.aps.org/supplemental/... for more information.

[25] R. Haussmann, W. Rantner, S. Cerrito, and W. Zwerger, Phys. Rev. A **75**, 023610 (2007).

[26] N. Navon, S. Nascimbne, F. Chevy, and C. Salomon, Science **328**, 729 (2010).

[27] K. M. O'Hara, S. L. Hemmer, M. E. Gehm, S. R.

Granade, and J. E. Thomas, Science **298**, 2179 (2002).
[28] L. Luo and J. Thomas, J. Low Temp. Phys. **154**, 1 (2009).
[29] M. J. H. Ku, A. T. Sommer, L. W. Cheuk, and M. W. Zwierlein, Science **335**, 563 (2012).